Phase diagram for the one-dimensional Hubbard-Holstein model: A density-matrix renormalization group study

Masaki Tezuka,[1,*] Ryotaro Arita,[2] and Hideo Aoki[1]

[1]*Department of Physics, University of Tokyo, Hongo, Tokyo 113-0033, Japan*
[2]*RIKEN, Wako, Saitama 351-0198, Japan*

Phase diagram of the Hubbard-Holstein model in the coexistence of electron-electron and electron-phonon interactions has been theoretically obtained with the density-matrix renormalization group method for one-dimensional systems, where an improved warm-up (the recursive sweep) procedure has enabled us to calculate various correlation functions. We have examined the cases of (i) the systems half-filled by electrons for the full parameter space spanned by the electron-electron and electron-phonon coupling constants and the phonon frequency, (ii) non-half-filled system, and (iii) trestle lattice. For (i), we have detected a region where both the charge and on-site pairing correlations decay with power laws in real space, which suggests a metallic behavior. While pairing correlations are not dominant in (i), we have found that they become dominant as the system is doped in (ii) or as the electronic band structure is modified (with a broken electron-hole symmetry) in (iii) in certain parameter regions.

I. INTRODUCTION

In condensed-matter physics, the electron-phonon interaction and electron-electron interaction are two of the fundamental interactions. While the problem is hard enough even when only one of them exists, it is a most challenging problem to consider what happens when both of the interactions coexist.

A central problem is the ground-state phase diagram—how various phases arise in the coexistence of two kinds of interactions that are quite different in nature. Of particular interest is superconductivity. Strong electron-electron repulsive interactions introduce spin fluctuations in the electronic system, which can mediate pairing interactions for the electrons to make them condense into superconducting states with anisotropic Cooper pairs.[1] The superconducting phase has to, however, compete with density-wave phases such as the spin-density wave (SDW), which also come from the electron-electron interaction.[2] On the other hand, the electron-phonon interaction mediates an attraction between electrons, which can make the electrons condense into superconducting states with isotropic Cooper pairs. This time the superconducting phase has to compete with density-wave phases such as the charge-density wave (CDW) arising from the electron-phonon interaction. The electron-phonon interaction is the coupling of the conduction electrons to the lattice structure, and it can also work to make the system undergo a Peierls transition, where the lattice is deformed so that the electrons are not conducting.

So it is quite a nontrivial problem to consider the ground-state phases when the two interactions coexist and are both strong. A prototypical model representing such a situation is the Hubbard-Holstein model, where the Hubbard model for the electron correlation is coupled to (Einstein) phonons. The model is characterized by three physical parameters: (a) the on-site electron-electron repulsion U, (b) the phonon frequency ω_0, and (c) the electron-phonon coupling λ, where the unit of energy is the electronic transfer $t \propto$ electronic

bandwidth W. Of particular interest is the intermediate regimes: (a) the regime $(\hbar\omega_0 \sim t)$ intermediate between the adiabatic $(\hbar\omega_0 \ll W)$ and antiadiabatic $(\hbar\omega_0 \gg W)$ limits; (b) the regime $(U \sim \lambda)$ where the electron-electron Coulomb repulsion and the phonon-mediated attraction are similar in magnitude. The problem has, in fact, been studied in various approaches.[3–26]

This is by no means a theoretical curiosity, since there are various classes of materials in which both the electron-electron and electron-phonon interactions are simultaneously strong. A typical example is the solid fullerene doped with alkali-metal atoms $(A_3C_{60}, A=K, Rb, etc.)$,[27–29] where the C_{60} fullerene molecules are aligned in a face-centered cubic (fcc) lattice, for which the alkali atoms supply electrons making the conduction band half-filled. In this material, the intramolecular phonon modes are known to have high frequencies $(\sim 0.2$ eV$)$, which couple strongly to the conduction electrons. The material is a superconductor whose transition temperature T_C is the highest to date among the carbon compounds. It is an interesting problem to consider how the half-filled electron band becomes metallic, rather than becoming CDW or SDW insulators from coexisting electron-electron and electron-phonon interactions, and exhibits superconductivity. The electronic bandwidth of A_3C_{60} can be controlled by, e.g., changing the alkali-metal species A, where T_C is observed to increase with the lattice constant. Organic chemists have also fabricated fullerene derivatives in the shape of a shuttlecock, where the molecules stack to form an array of one-dimensional (1D) chains,[30] where the separation between C_{60} molecules in a chain is controllable with the choice of functional groups attached to C_{60}, and the system is shown to have stronger electron correlation.[31]

Given these backgrounds, the purpose of the present paper is to obtain the ground-state phase diagram when the electron-phonon and electron-electron interactions coexist over the whole parameter space spanned by U, λ, $\hbar\omega_0$ that includes the intermediate regimes $(\hbar\omega_0 \sim W; U \sim \lambda)$. We adopt the Hubbard-Holstein model, one of the simplest mod-

els for the coexisting electron-electron and electron-phonon interactions. We want to treat these interactions on an equal footing, especially in the intermediate regimes. Phonons mediate attraction between electrons, but here we have adopted the dispersionless, Einstein phonons that do not directly propagate along the chain. While these phonons cannot directly mediate the pairing force between electrons across different sites, we can still expect the phonons to contribute to the pairing, because electrons hop between neighboring sites. So the phonon self-energy $\Sigma(q, \omega)$ should depend not only on ω but also on q. Specifically, phonons with $q \sim \pi/a$ (a: the lattice constant) as well as phonons with $q \sim 0$ should be strongly renormalized by the coupling to the electrons, because the Fermi points reside at $k = \pm \pi/2a$. This is another reason why the electron and phonon degrees of freedom should be treated on an equal footing.

So a special care has to be taken in choosing the method, since the method has to (a) take account of the phonons without assuming the adiabatic or antiadiabatic limits, and (b) take account of the electrons where charge gaps around the half-filled electronic band (a region of interest) can be described. We have adopted the density-matrix renormalization group (DMRG) as an appropriate method.

DMRG was originally developed for spin systems[32,33] and applications to electron systems subsequently followed.[34,35] The basic idea is the following: We iteratively add sites to enlarge a one-dimensional system, which is approximately represented as two connected *subchains* with truncated Hilbert spaces optimized for a target state of the whole system. In adding a site to a subchain, we calculate the partial density matrix for the target state wave function, diagonalize it, and retain eigenstates that correspond to a limited number of largest eigenvalues, to represent the new Hilbert space for the new subchain. While the DMRG was developed for electron systems, Jeckelmann and White extended the formalism to incorporate phonons in DMRG.[36] We have here adopted this formalism, with an improved algorithm.

In constructing a phase diagram, a most direct method is to actually calculate various correlation functions. However, the inclusion of phonons, which are bosons, makes the calculation enormously heavy, and we have to somehow overcome this difficulty. Here, we have adopted an improved warm-up (the recursive sweep) procedure for the DMRG developed by one of the present authors,[37] which has enabled us to actually calculate correlation functions (including the pairing correlation) for the Hubbard-Holstein model. While employment of 1D systems is a theoretical device (apart from the above mentioned quasi-1D fullerides), it is theoretically intriguing to look at functional forms of correlation functions in the coexistence of electron-electron and electron-phonon interactions. The Mermin-Wagner theorem dictates that continuous symmetries of the Hamiltonian are not broken in the ground states of infinite 1D systems. Hence, the correlation functions for the phases with broken continuous symmetry should decay with distance. We can still compare the exponents of the decay, as in the Tomonaga-Luttinger theory for purely electronic systems, to determine the dominant correlation, which may become long ranged once we go to higher dimensions.

Now, there are many existing theoretical studies on the Hubbard-Holstein model, but the nature of the model has yet to be fully established. There have been competing results even on the ground-state phase diagram at half-filling. Particular issues are as follows:

(1) For large enough U, we can expect the ground state to be a SDW, while for large enough λ, we can expect the ground state to be a CDW. An interesting problem is whether there exists a metallic phase between the two density-wave phases.

(2) Whether a naïve expectation is valid, where one imagines that, for the coexisting electron-electron and electron-phonon interactions, the net interaction will simply be the difference between them. This problem becomes especially interesting in the intermediate regime.

(3) Whether the metallic phase, if any, can possibly become superconducting. For pairing symmetries, we have here considered all the possibilities of the following:

    (a) sSC: on-site spin-singlet pairing,

    (b) pSC: nearest-neighbor spin-triplet pairing, and

    (c) dSC: nearest-neighbor spin-singlet pairing.

It may sound peculiar when we say p- or d-wave superconductivity for 1D systems, but a nearest-neighbor spin-triplet (singlet) pairing corresponds to a $p(d)$-wave pairing in two or higher dimensions, so we adopt this nomenclature.

(4) How the phase diagram depends on the electron band filling or the lattice structure (i.e., the electronic band structure) of quasi-1D systems.

In order to resolve these issues, we have obtained the correlation functions for long chains with DMRG for the cases of (i) the systems half-filled by electrons for the full parameter space spanned by the electron-electron and electron-phonon coupling constants and the phonon frequency, (ii) non-half-filled system, and (iii) trestle lattice. For (i), we have detected a region (where the electron-phonon interaction is stronger than U but not too strong) where both the charge and on-site (sSC) pairing correlations decay arithmetically in real space, which suggests a metallic behavior. While pairing correlations are not dominant in (i), we have found that they become dominant as the system is doped in (ii) or as the electronic band structure is modified (with a broken electron-hole symmetry) in (iii) in certain parameter regions.

Organization of the paper is as follows: In Sec. II, we introduce the Hubbard-Holstein model and briefly review the open questions about the phase diagram. In Sec. III, we explain the numerical method for calculating correlation functions. Results are presented in Sec. IV (half-filled chain), V (doped chain), and VI (undoped trestle lattice). Concluding remarks are given in Sec. VII.

II. MODEL

We take the Hubbard-Holstein model, where the electronic part of the Hamiltonian is the Hubbard model that in itself exhibits various phases according to the values of the electron band filling n and the short-range (on-site) electron-electron interaction U, dimensionality, and the lattice structure. Phonons are introduced as a local harmonic oscillator for each site, to which the electrons are coupled, as shown schematically in Fig. 1. Thus, the phonons are dispersionless
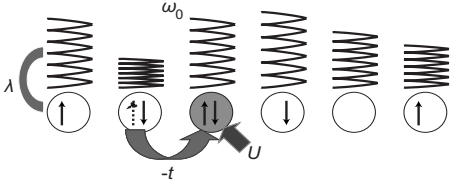
FIG. 1. The Hubbard-Holstein model. Each atom consists of an electron site (circle) and a local phonon with frequency ω_0 (spring). The arrows denote up and down spin electrons, which are coupled to the phonons with a strength λ. An electron can hop between neighboring sites with the hopping amplitude t and feel an on-site electron-electron repulsion U when encountered with another electron of opposite spin on the same site.

(i.e., Einstein phonons). Inclusion of on-site phonons adds two parameters to the Hubbard model: the electron-phonon coupling g and the phonon frequency ω_0. We can characterize the strength of the electron-phonon coupling,

$$\lambda \equiv 2g^2/\hbar\omega_0,$$

which is the attraction mediated by phonons between the two electrons on the same site in the antiadiabatic ($\omega_0/t \rightarrow \infty$) limit. We take this as the measure of the electron-phonon coupling to facilitate comparison with the electron-electron repulsion U. We set $\hbar = 1$ hereafter.

The Hamiltonian is given as

$$H = -\sum_{\langle i,j\rangle,\sigma} t_{ij}(c_{i\sigma}^{\dagger}c_{j\sigma} + c_{j\sigma}^{\dagger}c_{i\sigma}) + \sum_i U n_{i\uparrow}n_{i\downarrow}$$
$$+ \sum_{i,\sigma} g n_{i\sigma}(\tilde{a}_i + \tilde{a}_i^{\dagger}) + \sum_i \hbar\omega_0 \tilde{a}_i^{\dagger}\tilde{a}_i. \quad (1)$$

Here, $c_{i\sigma}$ annihilates an electron with spin $\sigma(=\uparrow,\downarrow)$ at site i, $n_{i\sigma} = c_{i\sigma}^{\dagger}c_{i\sigma}$ is the electron number, and $\tilde{a}_i$ is the phonon annihilator at site i. If we consider the phonon as a harmonic oscillator where a mass M is attached to a spring with a spring constant K with the phonon frequency $\omega_0 = \sqrt{K/M}$, the displacement x_i is written as

$$x_i = \frac{\hbar}{2M\omega_0}(\tilde{a}_i + \tilde{a}_i^{\dagger}). \quad (2)$$

The electron-phonon coupling is introduced as a coupling of the local electron number, $n_i \equiv \sum_\sigma n_{i\sigma}$, with the lattice displacement x_i.

The electron band filling is defined as $\bar{n}_\sigma = n/2$, and, by introducing $a \equiv \tilde{a} - g\bar{n}_\sigma/\hbar\omega_0$, we can rewrite Eq. (1), up to a constant, as

$$H = -\sum_{\langle i,j\rangle,\sigma} t_{ij}(c_{i\sigma}^{\dagger}c_{j\sigma} + c_{j\sigma}^{\dagger}c_{i\sigma}) + \sum_i U(n_{i\uparrow} - \bar{n}_\uparrow)(n_{i\downarrow} - \bar{n}_\downarrow)$$
$$+ \sum_{i,\sigma} g(n_{i\sigma} - \bar{n}_\sigma)(a_i + a_i^{\dagger}) + \sum_i \hbar\omega_0 a_i^{\dagger}a_i. \quad (3)$$

In this form, the relevant electron occupation is the deviation from the average value.

The Hubbard-Holstein model (1) has three independent parameters: $U/t, \lambda/t, \omega_0/t$, as schematically displayed in Fig. 2. In this parameter space, we are interested in the regimes
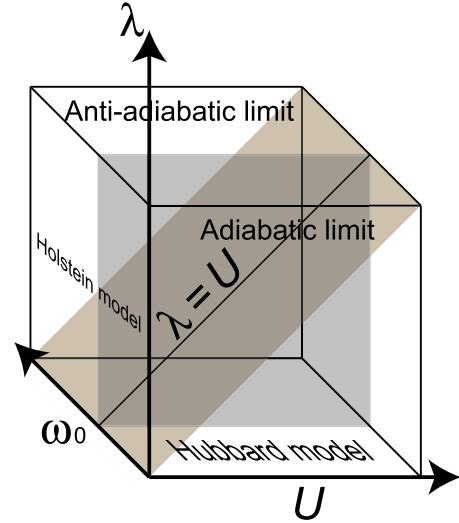

FIG. 2. (Color online) Parameter space for the half-filled Hubbard-Holstein model spanned by the on-site electron-electron repulsion U, the phonon frequency ω_0, and the electron-phonon coupling λ, where the unit of energy is the electronic transfer t. The model reduces to the Hubbard model when $\lambda = 0$, and to the Holstein model when $U = 0$. The $\omega_0/t \rightarrow 0$ limit is the adiabatic limit, while the $\omega_0/t \rightarrow \infty$ limit is the antiadiabatic limit.

(i) away from the adiabatic ($\omega_0/t \ll 1$) or antiadiabatic ($\omega_0/t \gg 1$) limits and (ii) comparable $U \sim \lambda$. To summarize the existing theoretical results on the 1D half-filled Hubbard-Holstein model, we observe the following issues:

(1) Two of the recent studies on this model, one with the Lang-Firsov transformation[21] and the other with DMRG,[22] have different conclusions as to where this model becomes metallic. The former indicates a considerably wide metallic region between the CDW ($U \ll \lambda$) and SDW ($\lambda \ll U$) phases, while the latter indicates a closing of the charge gap only at a quantum critical point between the CDW and SDW insulators.

(2) While the strong-coupling expansion[8] indicates that superconductivity cannot be dominant for finite ω_0, a study with some ansatz for phonons[6] indicates a dominant superconductivity near the $U = 0$ axis on the U-λ phase diagram, and another quantum Monte Carlo study for the charge structure factor[25] suggests a phase diagram with a superconducting region near the $U = \lambda$ line between the CDW and SDW phases.

On the other hand, the Holstein model corresponds to the $U = 0$ plane in the phase diagram of the Hubbard-Holstein model and picks up the effect of the electron-phonon interaction in making the electronic system insulating. In one[38,39] and two dimensions, and in the limit of infinite dimension,[40,41] there are extensive studies on the transition between (i) the small-polaron regime, where the electrons are self-trapped by the lattice through a stronger electron-phonon interaction, and (ii) the large-polaron regime, where the electrons move around exciting local phonons through a weak electron-phonon interaction.[42] When the electron-electron interaction is turned on in such an electron-phonon system, the interplay between the effects of the electron-phonon and

electron-electron interactions again becomes interesting, which has not been fully understood.

III. METHOD

As we have seen, the ground-state phase diagram for the 1D Hubbard-Holstein model is controversial. The most clear-cut way for examining the competition of various phases is to look at the correlation functions on long systems, which has not previously been done properly. So here we calculate correlation functions in real space. A care has to be taken in examining correlation functions in 1D quantum systems: strong quantum fluctuations repress continuous symmetry-broken long-range orders in the ground state.[43,44] However, if one type of correlation function decays more slowly than others, we can identify the correlation to be dominant. Exact results for purely electronic systems on various integrable models show that diagonal $[\langle c^\dagger(r)c(r)c^\dagger(0)c(0)\rangle]$ and pair $[\langle c^\dagger(r)c^\dagger(r)c(0)c(0)\rangle]$ correlations decay with a power law ($r^{-\eta}$, where η is an exponent) or exponentially ($e^{-r/\xi}$, where ξ is the correlation length) at large distances r.

In the case of charge and spin correlations, the charge (spin) correlation function decays with a power law when the charge (spin) excitation is gapless, $\Delta_{charge}=0$ ($\Delta_{spin}=0$), while the correlation decays exponentially when the charge (spin) excitation has a gap $\Delta_{charge}>0$ ($\Delta_{spin}>0$). To be precise, these correlations can have logarithmic corrections or additional terms that decay faster than the main term. This is one reason why we need long chains to identify the dominant phase by numerically calculating the decay of correlation functions. Here, we compare the real-space behavior of various correlation functions in the ground state for a chain having as many (typically 64) sites as numerical calculation is possible for model parameters away from the adiabatic and antiadiabatic limits. For these reasons, we adopt the DMRG with the pseudosite method[36] to calculate the ground-state correlations. We adopt the open-boundary condition for a better DMRG convergence. The recursive sweep initialization[37] adds two sites for both the electron and phonon degrees of freedom at each infinite-algorithm DMRG step, while benefiting from the reduced size of the Hilbert space in the pseudosite method. This also contributes to better convergence with less computational resources, which has allowed us to compute correlation functions on lattices with large number of sites.

IV. RESULT: HALF-FILLED HUBBARD-HOLSTEIN CHAIN

A. Parameter space

First, we investigate half-filled systems for the parameter space shown as a bird's eye view in Fig. 2 (with $t=1$ taken as the unit of energy), while the doped case is treated in Sec. V.

We calculate charge, spin, and pair correlation functions for this parameter space. For the pairing symmetry, we consider the on-site, spin-singlet pair (sSC) (which corresponds to s-wave superconductivity in higher spatial dimensions), spin-singlet pair across the neighboring sites (dSC) (d wave in higher dimensions), and triplet pair across neighboring
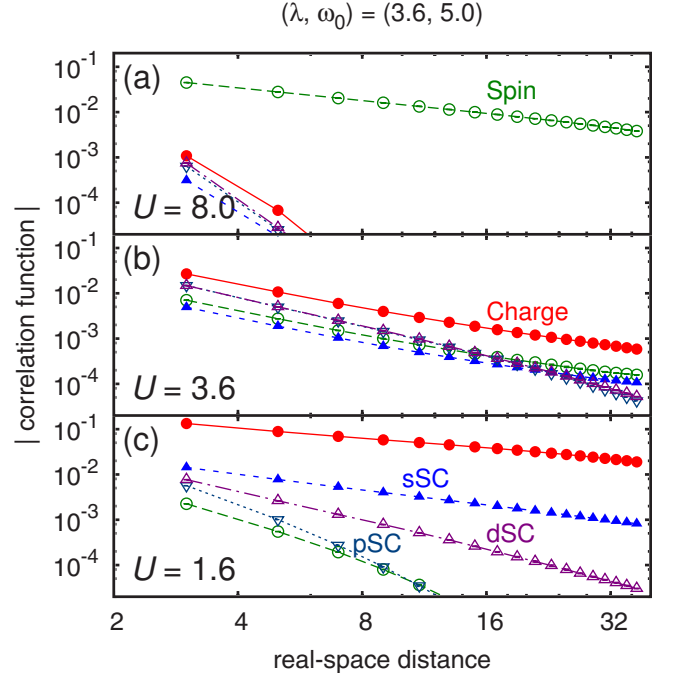

FIG. 3. (Color online) Log-log plot of correlation functions against the real-space distance for $(\lambda,\omega_0)=(3.6,5.0)$ and $U=$(a) 8.0, (b) 3.6, and (c) 1.6 for the half-filled Hubbard-Holstein model.

sites (pSC) (p wave in higher dimensions). Their operator forms are as follows:

(1) Charge: $\langle n_i n_j\rangle-\langle n_i\rangle\langle n_j\rangle$,

(2) spin: $\langle S_i^z S_j^z\rangle$,

(3) sSC: $\langle \Sigma_i^\dagger \Sigma_j\rangle$,

(4) pSC: $\langle \Pi_i^\dagger \Pi_j\rangle$, and

(5) dSC: $\langle \Delta_i^\dagger \Delta_j\rangle$, where $n_i\equiv\Sigma_\sigma n_{i\sigma}$, $S_i^z\equiv(n_{i\uparrow}-n_{i\downarrow})/2$, $\Sigma_i\equiv c_{i\uparrow}c_{i\downarrow}$, $\Pi_i\equiv(c_{i\uparrow}c_{i+1\downarrow}+c_{i\downarrow}c_{i+1\uparrow})/\sqrt{2}$, and $\Delta_i\equiv(c_{i\uparrow}c_{i+1\downarrow}-c_{i\downarrow}c_{i+1\uparrow})/\sqrt{2}$.

We first display typical dependence of correlation functions on the real-space distance along the chain. The calculations have been done on $L=64$-site, half-filled Hubbard-Holstein chains, with pseudosite DMRG for at least $N_b=3$ phonon pseudosites per full site, unless otherwise indicated. At least ten finite-system sweeps have been done with $m>400$ states retained in more than two final iterations after the infinite-finite method warm-up. The results do not change significantly when we take larger $N_b\geq4$ or $m>500$. The maximum discarded weight of the partial density matrix in the final sweep is below 10^{-5} when $m>400$ and typically around 10^{-7} when $m>500$.

B. Case of larger ω_0/t

First, we consider the region where the phonon frequency is greater than the electron hopping t. We fix the electron-phonon coupling λ and phonon frequency ω_0 at $(\lambda,\omega_0)=(3.6,5.0)$. We observe in Fig. 3(a) that only the spin correlation decays with a power law for U much larger than λ. The exponent is near unity.

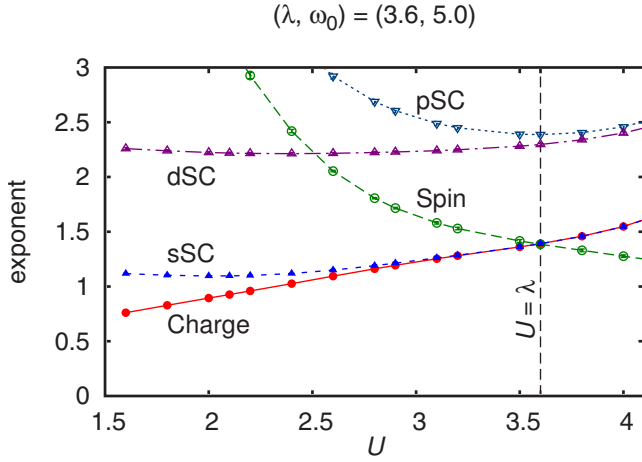As U is decreased to around λ, the charge correlation begins to decay with a power law, as plotted in Fig. 3(b) for

FIG. 4. (Color online) Exponents of correlation functions for the Hubbard-Holstein model with $(\lambda, \omega_0) = (3.6, 5.0)$.
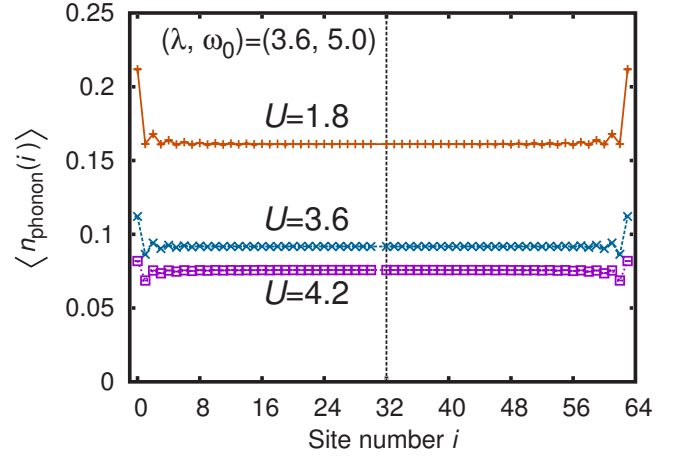

FIG. 5. (Color online) Phonon number $\langle n_{\mathrm{phonon}}(i) \rangle$ plotted against i for $U = 1.8, 3.6, 4.2$ and $(\lambda, \omega_0) = (3.6, 5.0)$ for a 64-site, half-filled Hubbard-Holstein chain.

$U = 3.6 = \lambda$. The exponent for the spin correlation is greater than in Fig. 3(a). Here, we note that the on-site pair correlation also decays with a power law.

Finally, for a much smaller value of $U = 2.6$ in Fig. 3(c), the spin correlation decays no longer with a power law, but almost exponentially at large distances, which becomes more manifest as U is further decreased. There, both CDW and on-site pair correlations still decay with power laws. So we observe a power law spin correlation when the electron-electron interaction is stronger than the electron-phonon interaction, or power-law charge and on-site pair correlations when the electron-electron interaction is weaker.

Next, we compare the exponents of the correlations. We fit the correlations as functions of the real-space distance r, assuming the behavior $\langle O^\dagger(x) O(x+r) \rangle \sim r^{-\eta}$, and determine the exponent η. The results are plotted in Fig. 4. We can see that charge and on-site pair correlations have similar exponents, but the exponent for the charge correlation is always smaller than that for the on-site pair correlation. So the charge correlation is dominant when U/t is smaller than around 3.5 where $\lambda = 3.6$, while the spin correlation is dominant when U/t is larger.

For the repulsive ($U > 0$) Hubbard model, we have only the spin correlation decaying as r^{-1}. Now, for the purely electronic Hubbard model, it has been known[45,46] that we can convert the repulsive ($U > 0$) Hubbard model into the attractive ($U < 0$) Hubbard model, at half-filling, with a canonical transformation, with which the charge and sSC pair correlations are mapped to the spin correlation in the repulsive side as

$$U \leftrightarrow -U$$

$$\langle (n_{i\uparrow} + n_{i\downarrow})(n_{j\uparrow} + n_{j\downarrow}) \rangle \leftrightarrow \langle (n_{i\uparrow} - n_{i\downarrow})(n_{j\uparrow} - n_{j\downarrow}) \rangle \propto \langle S_i^z S_j^z \rangle$$

$$\langle c_{i\downarrow} c_{i\uparrow} c_{j\uparrow}^\dagger c_{j\downarrow}^\dagger \rangle \leftrightarrow \langle c_{i\downarrow} c_{i\uparrow}^\dagger c_{j\uparrow}^\dagger c_{j\downarrow} \rangle \propto \langle S_i^- S_j^+ \rangle. \quad (4)$$

This implies that the charge and sSC pair correlations are degenerate and both decay like r^{-1} as far as the Hubbard

model ($U < 0$) and the Hubbard-Holstein model ($\tilde{U} \equiv U - \lambda < 0$) in the antiadiabatic limit are concerned.

If we go back to the Hubbard-Holstein model, the power-law fit for an exponentially decaying correlation gives a finite exponent for finite systems, so what we should observe when a correlation does become power law is a decrease of the exponent around the phase transition point. We observe in Fig. 4 that the exponent for the SDW (CDW and sSC) decreases (increases) as $\tilde{U} \equiv U - \lambda$ is increased from the negative to positive sides. This behavior is similar to the Hubbard model having $\tilde{U}$ as the on-site interaction, except that the exponent for the charge correlation is slightly smaller than that of the sSC pair correlation in general for finite ω_0/t as mentioned above. This is similar to the case of the Holstein model $U = 0$ with an $\omega_0/t \sim 5$ (not shown).

C. Phonon numbers per site in the Hubbard-Holstein model

We can calculate the phonon occupation number for each site $n_{\mathrm{phonon}}(i)$ in the ground state ψ_0, defined as

$$\langle n_{\mathrm{phonon}}(i) \rangle \equiv \langle \psi_0 | a_i^\dagger a_i | \psi_0 \rangle. \quad (5)$$

We can check the boundary effects by plotting the phonon number against the site number i in Fig. 5. The curves are almost flat except for a few sites around either edge of the chain.

We plot the phonon number at the center of the chain, $\langle n_{\mathrm{phonon}} \rangle$, as a function of U in Fig. 6(f). Phonons mediate an attraction between the two electrons with opposite spins on the same site, which amounts to $\lambda \equiv 2g^2/\omega_0$ in the $\omega_0 \to \infty$ limit. For a finite ω_0, the attraction λ is smaller than this asymptote λ.[47,48] For $U \ll \lambda$, two electrons tend to form a bipolaron, where the electrons are strongly bound to each other by sharing phonons they excite. Bipolarons, at half-filling, tend to occupy every second site to reduce kinetic energy. In this case, the charge correlation that corresponds to the $2k_F$ CDW is the strongest. The number of excited
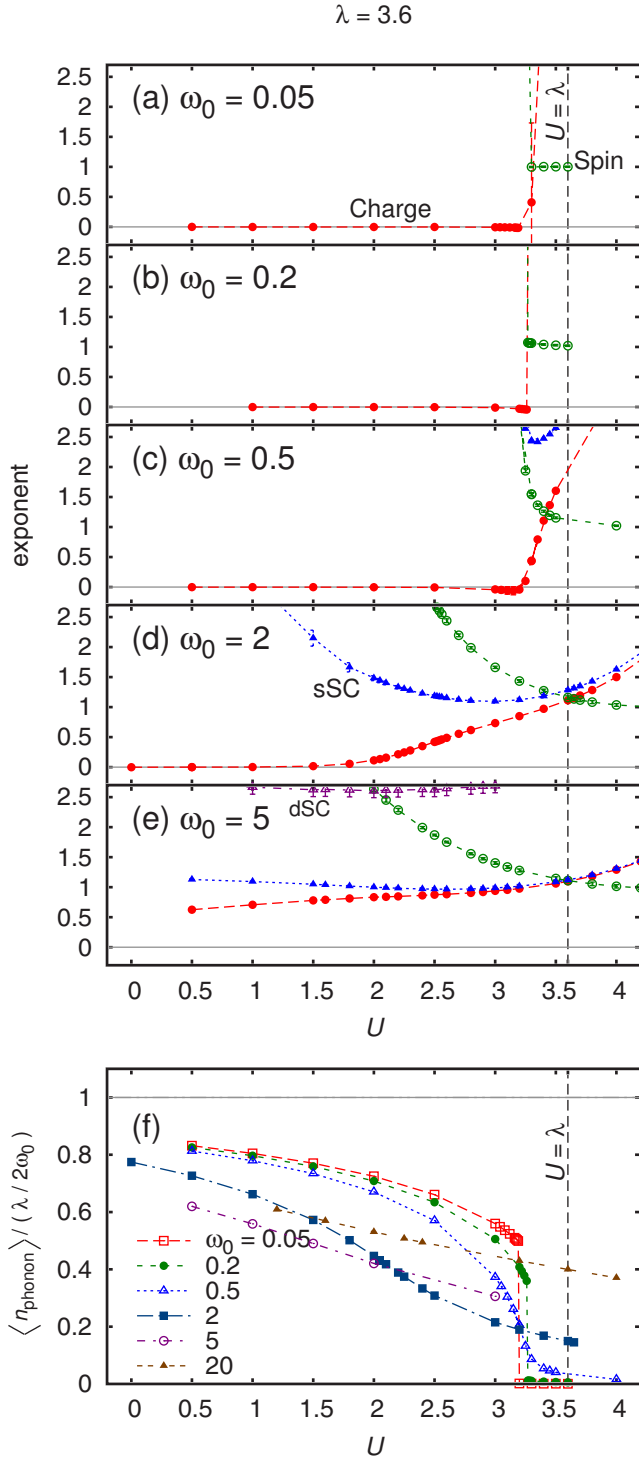
FIG. 7. (Color online) Correlation functions for (U, λ, ω) $= (2.1, 3.6, 2.0)$ on a 64-site, half-filled Hubbard-Holstein chain with $N_b = 6$, where CDW correlation is dominant and almost constant.

mation $\hat{a} = a - \sqrt{\alpha}$. Then the local Hamiltonian for the phonon on this site is

$$H = g(a + a^\dagger) + \omega_0 a^\dagger a = \omega_0 \hat{a}^\dagger \hat{a} + (\omega_0 \alpha + 2g\sqrt{\alpha}), \quad (6)$$

with $\alpha \equiv (g/\omega_0)^2 = \lambda/2\omega_0$. The second term is a constant, and if we denote the n-phonon state as $|n\rangle$ $(n = 0, 1, \ldots)$, the ground state $|\psi_0\rangle = \Sigma_n b_n |n\rangle$ satisfies

$$\hat{a}|\psi_0\rangle = (a - \sqrt{\alpha}) \sum_n b_n |n\rangle = \sum_{n \geq 1} (\sqrt{n} b_n - \sqrt{\alpha}) |n - 1\rangle = 0.$$

$$(7)$$

This is solved as a coherent state,

$$b_n = \sqrt{e^{-\alpha} \alpha^n / n!}, \quad (8)$$

which gives

$$\lim_{U \to 0} \langle n_{\text{phonon}} \rangle = \langle a^\dagger a \rangle = \frac{\displaystyle\sum_{n \geq 1} \alpha^n/(n-1)!}{\displaystyle\sum_{n \geq 0} \alpha^n/n!} = \alpha = \lambda/2\omega_0. \quad (9)$$

We can observe in Fig. 6(f) that the system indeed approaches to this limit as U is decreased.

A deviation observed for larger values of ω_0 in Fig. 6(f) is interesting in that the region is intermediate between the $U \ll \lambda$ and $U \gg \lambda$ limits. There we can expect a behavior different from the limiting behavior.

D. Case of smaller ω_0/t

When the value of ω_0/t is smaller than about 3, we start to observe in Fig. 6(c) behaviors of the correlation functions different from those discussed above: the value of U at which the exponent for the charge and spin correlations coincide becomes considerably smaller than λ. So the $(U - \lambda)$ Hubbard model picture is *no longer valid*. Secondly, the charge correlation becomes almost flat against distance as in Fig. 7, implying a charge-ordered (CO) phase, in some region of U in Figs. 6(a)–6(d), while this does not happen for the on-site pair correlation.

To analyze the nature of this behavior, we can again look at the phonon occupation number against U for various val-

FIG. 6. (Color online) [(a)–(e)] Exponents of correlation functions determined by calculating exponents for a 20-site Hubbard-Holstein model for $\lambda/t = 3.6$ with various values of $\omega_0/t = 0.05 - 5$. (f) The phonon number per site, normalized by Eq. (9).

phonons per site increases as U is decreased, because the fluctuation from the single occupancy increases as the CDW correlation becomes stronger.

The limit of immobile bipolarons can be understood as follows: we consider two electrons on a site in Eq. (3) and neglect their hopping, to apply a Lang-Firsov-type transfor-
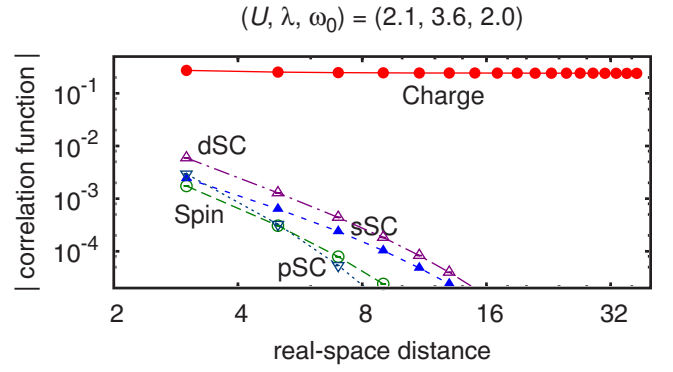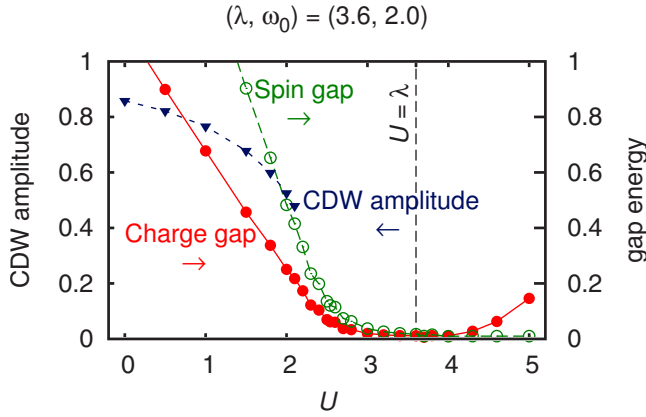
FIG. 8. (Color online) Charge gap, spin gap, and CDW amplitude plotted against U for the half-filled Hubbard-Holstein model with $(\lambda, \omega_0) = (3.6, 2.0)$. Data obtained for $L = 20, 30, 40, 64$ have been linearly extrapolated to $1/L \to 0$.

TABLE I. Summary of possible phases at half-filling. We denote power-law and exponential decays of correlation functions ("corr.") as "power" and "exp.," respectively.

Phase	CO	CDW/sSC	SDW
Spin corr.	Exp.	Exp.	Power
Charge corr.	Long-range order	Power (smallest η)	Exp.
sSC corr.	Exp.	Power	Exp.
Charge gap	Finite	0	Finite
Spin gap	Finite	Finite	0
$\langle n_{\text{phonon}} \rangle$	$\to \lambda/2\omega_0$	Intermediate	$\to 0$

ues of ω_0 for a fixed value of λ [Fig. 6(f)]. For small enough ω_0, the phonon occupation number abruptly increases at some value U_c as U is decreased. We can see that the exponential decay of all the correlations except the charge correlation, in fact, starts around $U = U_c$. Thus, we identify that this is where the SDW-CDW transition occurs. For larger ω_0, on the other hand, the changes in both the exponents and the phonon occupation number are gradual. The intermediate values $(0 < \langle n_{\text{phonon}} \rangle < \lambda/2\omega_0)$ of the phonon occupation number is consistent with the power-law behavior of the CDW and sSC exponents, which corresponds to a metallic phase with a closed charge gap, where the fluctuation in the local electron number (hence the fluctuation in the local phonon number) will be large.

When we look at the CDW correlation,

$$\xi_{\text{charge}}(i,j) \equiv \left\langle \psi_0 \left| \left(\sum_\sigma n_{i\sigma} \right) \left(\sum_\sigma n_{j\sigma} \right) \right| \psi_0 \right\rangle - 1, \quad (10)$$

its amplitude turns out to either decay or remain almost constant (ξ_{CO}) against the distance $r = |i - j|$. Since $\langle \sum_\sigma n_{i\sigma} \rangle$ alternates between $1 + f_{\text{CO}}$ and $1 - f_{\text{CO}}$ in the latter case at half-filling, we can simply define the charge-ordering amplitude $f_{\text{CO}} = \sqrt{|\xi_{\text{CO}}|}$. We plot Δ_{charge}, Δ_{spin}, and f_{CO} against U in Fig. 8. As U is decreased in the CO region, we observe that (i) the CDW amplitude f_{CO} increases and approaches unity, (ii) both the spin and charge gaps increase almost linearly, and (iii) the spin gap is nearly twice the charge gap. For the CDW/sSC region, the charge gap almost vanishes. The spin gap becomes also small, but remains larger than the charge gap. Finally, when U exceeds λ, the spin gap remains zero, while the charge gap slightly grows with U.

The effect of the ratio ω_0/t on the U dependence of $\langle n_{\text{phonon}} \rangle$ can now be understood in the limits of $\omega_0 \gg t$ and $\omega_0 \ll t$ as follows:

(1) In the antiadiabatic limit ($\omega_0 \gg t$), the response of the phonons to the motion of electrons is so fast that we can think of the role of phonons as just mediating the attraction λ between electrons. Electrons then tend to occupy different sites for $U > \lambda$, with spins antiparallel between the neighbors

because of the exchange interaction. In this case, the spin correlation that corresponds to the $2k_F$ SDW is the strongest, and the number of excited phonons per site decreases with U, because the electron occupancy becomes closer to unity for every site.

(2) In the adiabatic limit ($\omega_0 \ll t$), for $U \ll \lambda$ the deviation (f_{CO}) of the electron occupancy from the average value is large, so that a larger number of phonons are excited. The dynamics of phonon is much slower than that of electrons for $\omega_0 \ll t$, and exactly when the charge-ordered states exist depends on ω_0 as we shall show on the phase diagram. For $U \gg \lambda$ electrons cannot move and form a Mott insulator, so that phonons are hardly excited. In the region $\omega_0 \lesssim t$, we observe a jump in $\langle n_{\text{phonon}} \rangle$ as a function of U. This should correspond to the CDW transition.

E. Phase diagram

As we have seen above, we have two to three distinguishable regions out of the five phases compared in Table I when we increase the value of U from $U = 0$:

(1) Charge ordering ($\Delta_{\text{spin}} \sim \Delta_{\text{charge}} > 0$). The charge correlation is dominant and does not exhibit a significant decay against distance. Other correlation functions decay exponentially. The charge and spin gaps are still large, but decrease with U. These should be the characteristics of a long-range charge order, which is not forbidden from Refs. 43 and 44. We denote this region as CO.

(2) CDW/sSC ($\Delta_{\text{charge}} \ll t$, $0 < \Delta_{\text{spin}} \ll t$). The charge and sSC correlations decay with power law, with the charge correlation the stronger of the two. The spin gap is finite (although a size-scaling argument will be required to quantify this), while the charge gap is closed (although a size-scaling argument will again be required). We denote this region as CDW/sSC because the sSC correlation, while not dominant anywhere, decays with power law as well. The dSC correlation (nearest-neighbor spin-singlet pair) is even less dominant.

(3) SDW ($\Delta_{\text{charge}} > 0$, $\Delta_{\text{spin}} \ll t$). Only the spin correlation decays with power law with the exponent being nearly unity. The spin gap is closed or much smaller than t. The charge gap becomes larger as U is increased. We denote this region as SDW.

We draw phase diagrams on the U-λ plane for various values of $\omega_0 = 0.2, 0.5, 2$, and on the U-ω_0 plane for various
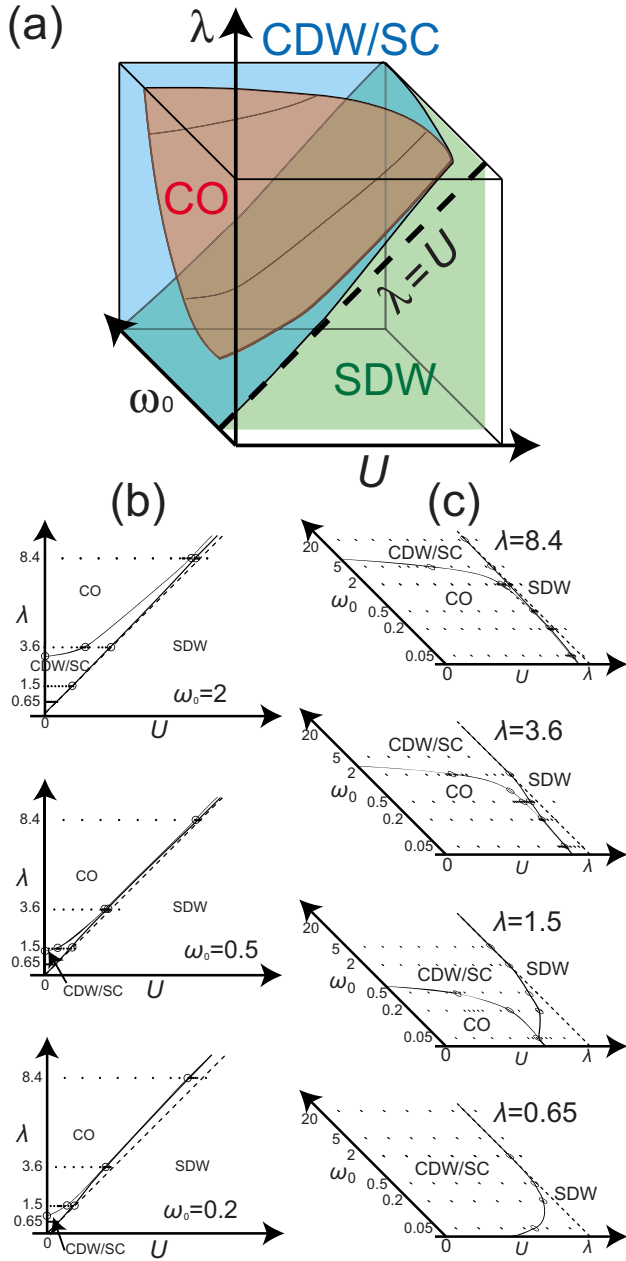
FIG. 9. (Color online) (a) The summary phase diagram on the whole parameter space for the half-filled Hubbard-Holstein model as derived from (b) the results obtained for the U-λ cross sections and (c) U-$\log \omega_0$ cross sections. The boundaries have been determined from the data points marked with dots.

values of $\lambda = 0.65, 1.5, 3.6, 8.4$ [Figs. 9(b) and 9(c)]. We observe on the U-ω_0 plane that the CDW/SC region is narrow for $\omega_0 \ll \lambda$, while the region expands with the CO-CDW/SC boundary shifting to smaller U and the CDW/SC-SDW boundary shifting to larger U, until the region finally extends up to $U \sim \lambda$ when $\omega_0 \gtrsim \lambda$. The CO region also becomes wider for smaller ω_0 or smaller U, but vanishes at $\omega_0 \sim \lambda$. For $\lambda = 0.05$, we have not detected this region.

On the U-λ plane, we observe that the SDW region covers all of $U > \lambda$, but it extends beyond the line $U = \lambda$ when ω_0 is smaller. The CDW/sSC region is broader for larger values of
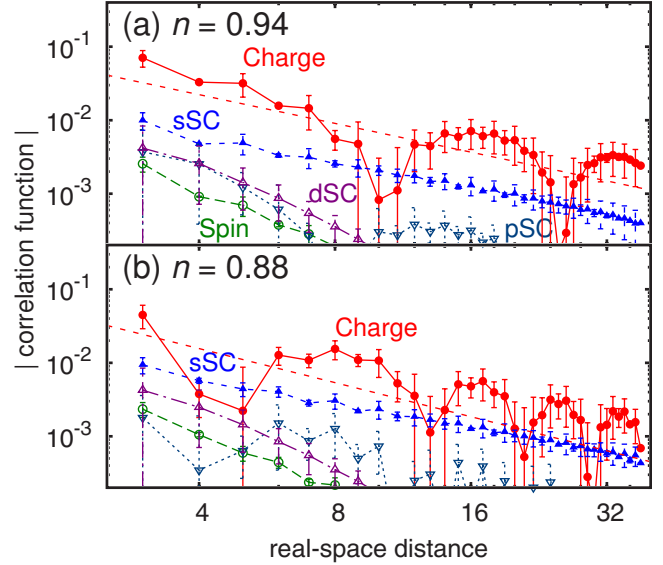

FIG. 10. (Color online) Correlation functions for a 64-site, *hole-doped* [$n = 60/64 = 0.94$ in (a) and $n = 56/64 = 0.88$ in (b)] Hubbard-Holstein chain with $(U, \lambda, \omega_0) = (2.0, 3.6, 5.0)$. The exponents for the sSC correlation (dotted straight line) are estimated to be $\eta_{sSC} = 1.16 \pm 0.02$ in (a) and $\eta_{sSC} = 1.09 \pm 0.02$ in (b), while the CDW correlation to be $\eta_{CDW} = 1.30 \pm 0.10$ in (a) and $\eta_{CDW} = 1.54 \pm 0.13$ in (b).

ω_0, and we have not detected CO region for $\omega_0/t = 20$. Figure 9(a) summarizes the whole region.

V. DOPED CHAIN

Having seen that the pairing correlation is only subdominant in the half-filled Hubbard-Holstein model, we can naturally ask the question: can the system away from the half-filling be superconducting? Since the effect of doping is dramatic in purely electronic systems such as the Hubbard model, this is an obviously interesting avenue to examine. For the doped systems, we change in our DMRG calculation the target quantum number, which is the pair of the spin up and the spin down electrons $(N_\uparrow, N_\downarrow)$, and change the values of $\bar{n}_\sigma$ in Eq. (3) accordingly.

The functional forms of the correlations for the non-half-filled system have turn out to have the following property: the pair correlation functions decay almost exactly with a power law, while the charge correlation decays as a power law multiplied by an oscillating factor. The dominant wave number for the CDW correlation should be $2k_F$, which equals to π/a (a: the lattice constant) at half-filling, but becomes larger as the hole doping is increased. In fact, we can fit the result for the CDW correlation as

$$\xi_{CDW} \simeq C r^{-\eta_{CDW}} \cos(qr + c), \quad (11)$$

where η_{CDW} is the exponent, C, c, and $q(\simeq n\pi/a)$ are fitting parameters.

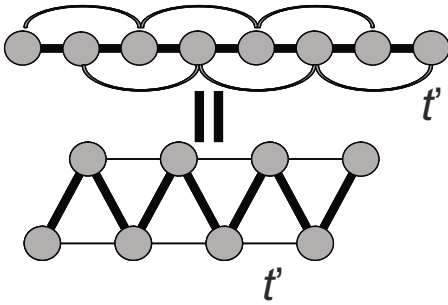We compare the CDW exponent thus obtained with the exponent for the sSC correlation (dashed line) in Fig. 10. The

FIG. 11. (Color online) A trestle lattice (bottom) is equivalent to a chain that has the next-nearest-neighbor hopping t' (top).

calculated exponents for CDW and sSC are similar in Fig. 10(a), where the electron filling n is close to unity. However, sSC becomes clearly dominant over CDW for a larger level of hole doping ($n=0.88$) in Fig. 10(b). The exponents in this case are $\eta_{sSC}=1.09\pm0.02$ and $\eta_{CDW}=1.54\pm0.13$. So this is the key result for the doped system: the sSC correlation has a smaller exponent and thus dominant in the sufficiently doped case.

In two or higher dimensions, superconductivity in the doped Hubbard-Holstein model poses an interesting problem, especially because the simplified $\tilde{U}\equiv U$-λ picture can be invalidated as stressed above. So this should be a further avenue for future studies.

VI. EFFECT OF THE LATTICE STRUCTURE: TRESTLE LATTICE

A second approach to make the pairing correlation dominant should be, in our view, to modify the electronic band structure. Along the line of argument above, we can specifically break the electron-hole symmetry to lift the degeneracy between the CDW and sSC correlations, Eq. (4), which exists in the Hubbard model[46] and is shown above to persist for the Hubbard-Holstein model in the antiadiabatic limit. This can be done by considering quasi-1D lattices such as ladder or trestle lattices. A trestle lattice, for instance, is equivalent to a chain where a next-nearest-neighbor hopping t' is introduced (Fig. 11). This washes out the bipartite symmetry in the band structure, which in turn breaks the electron-hole symmetry. We can then seek the possibility of making the pairing correlation dominant, even at half-filling, in the Hubbard-Holstein model, as have been done for the Hubbard model.[49,50]

So we have performed the DMRG study for the trestle lattice. We retained up to $m=720$ states per block. The maximum truncation error in the final sweep is around 10^{-5}, so it is considerably larger than in the case of the simple chain. If we look at the correlation functions against the real-space distance in Fig. 12, we can see that the sSC correlation is indeed dominant at $(U,\lambda,\omega_0,t')=(2.5,3.6,5.0,-0.4)$, even though we consider a half-filled system. Here, both of the charge correlation (at r = odd distances) and sSC correlation functions exhibit power-law decay. We can then look at the exponents of correlation functions against U for various val-

ues of t'/t, which control the band structure (top insets of Fig. 14). A special interest is that the number of Fermi points at half-filling for the noninteracting system increases from 2 to 4 at $|t'|>0.5$. Curiously enough, the case of four Fermi points is seen in the bottom panel of Fig. 13 to have a dominant dSC correlation for $U\ll\lambda$. This is the key results for the trestle lattice.

For $U\sim\lambda$, we observe relatively larger error bars in the exponents. This should be due to the presence of four Fermi points, for which we have a larger number of k points around E_F in a finite system. When $U\gg\lambda$, dominance of the SDW is recovered as in the case of the 1D chain and trestle lattice with smaller $|t'|$.

Next, we plot the exponents of the correlation functions as functions of t' in Fig. 14. The vertical dashed line in the figure represents the boundary at which the number of Fermi points changes from 2 to 4. In other words, a geometrical frustration (i.e., interference between the nearest-neighbor

Trestle, $(U, \lambda, \omega_0,t') = (2.5, 3.6, 5.0, -0.4)$, $n = 1$
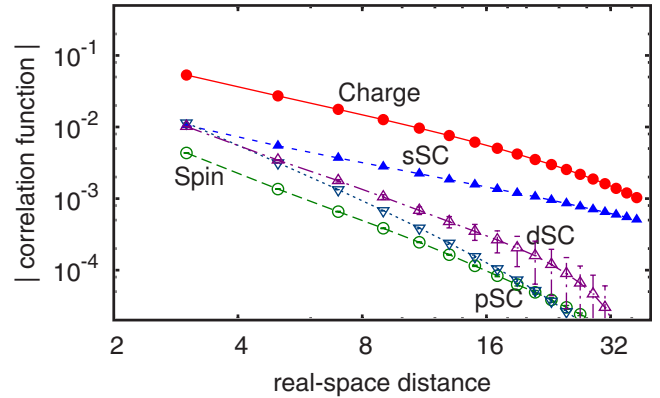
FIG. 12. (Color online) Correlation functions plotted against the real-space distance r for a 64-site, half-filled Hubbard-Holstein model on the trestle lattice with $(U,\lambda,\omega_0,t')=(2.5,3.6,5.0,-0.4)$.

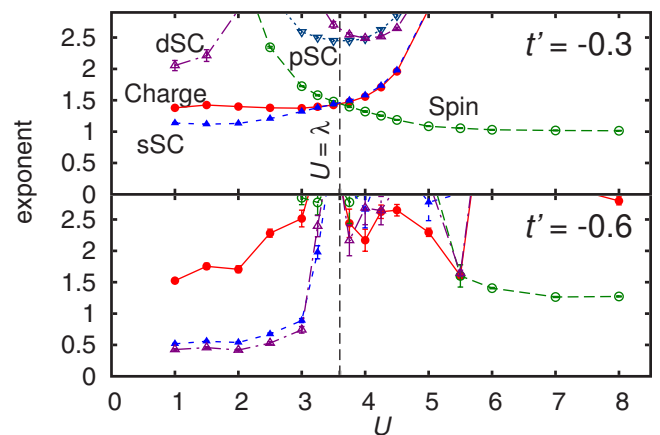Trestle, $(\lambda, \omega_0) = (3.6, 5.0)$, $n=1$

FIG. 13. (Color online) Exponents of correlation functions plotted against U for a 64-site, half-filled Hubbard-Holstein model on the trestle lattice for $(\lambda,\omega_0)=(3.6,5.0)$ with $t'/t=-0.3$ (top panel) or -0.6 (bottom).
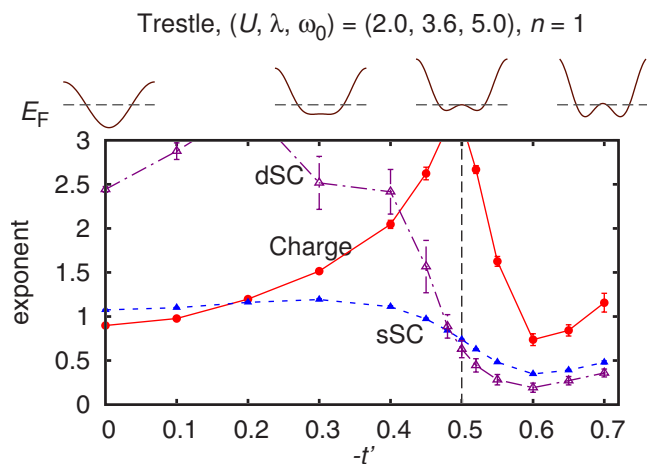
FIG. 14. (Color online) Correlation exponents plotted against $-t'$ for a 40-site, half-filled Hubbard-Holstein model on the trestle lattice with $(U, \lambda, \omega_0) = (2.0, 3.6, 5.0)$. At least $m = 630$ states have been retained in the last (tenth) sweep of the finite algorithm DMRG. The vertical dashed line represents the boundary at which the number of Fermi points changes from 2 to 4 as indicated by the band dispersion (top insets).

and second-neighbor transfers) becomes the strongest around this boundary. We can notice that the pairing correlations (sSC and dSC) tend to be dominant around the boundary, while the CDW correlation begins to decay faster there.

VII. SUMMARY

To summarize, we have shown for the 1D Hubbard-Holstein model the following: (i) For the half-filled case, we have obtained the phase diagram for the whole parameter space spanned by the Hubbard U, phonon frequency ω_0, and the electron-phonon coupling λ. A region is shown to exist between the SDW and CO phases, where the superconducting correlation is only subdominant against CDW. (ii) When we either (a) dope the electronic band or (b) change the electronic band structure by considering a trestle lattice, the on-site pair correlation, and in the case of (b) the nearest-site singlet pair correlation, indeed become dominant over CDW. This is to be contrasted with the Tomonaga-Luttinger picture (g ology), which would dictate that the pair correlation should not dominate when there are two Fermi points (the region left of the dashed line in Fig. 14).

*Present address: Department of Physics, Tokyo Institute of Technology, Ookayama, Tokyo 152-8551, Japan. tezuka.m.aa@m.titech.ac.jp

[1] V. J. Emery, Phys. Rev. Lett. **58**, 2794 (1987).

[2] J. R. Schrieffer, X.-G. Wen, and S.-C. Zhang, Phys. Rev. Lett. **60**, 944 (1988).

[3] G. Beni, P. Pincus, and J. Kanamori, Phys. Rev. B **10**, 1896 (1974).

[4] B. Horovitz, Phys. Rev. B **16**, 3943 (1977).

[5] J. E. Hirsch and E. Fradkin, Phys. Rev. B **27**, 4302 (1983).

[6] F. Guinea, J. Phys. C **16**, 4405 (1983).

[7] L. G. Caron and C. Bourbonnais, Phys. Rev. B **29**, 4230 (1984).

[8] J. E. Hirsch, Phys. Rev. B **31**, 6022 (1985).

[9] J. Voit and H. J. Schulz, Phys. Rev. B **34**, 7429 (1986); **37**, 10068 (1988).

[10] K. Nasu, Phys. Rev. B **35**, 1748 (1987).

[11] G. T. Zimanyi, S. A. Kivelson, and A. Luther, Phys. Rev. Lett. **60**, 2089 (1988).

[12] J. Voit, Phys. Rev. Lett. **64**, 323 (1990).

[13] H. Zheng, D. Feinberg, and M. Avignon, Phys. Rev. B **41**, 11557 (1990).

[14] Y. Takada, J. Phys. Soc. Jpn. **65**, 1544 (1996).

[15] K. Yonemitsu and M. Imada, Phys. Rev. B **54**, 2410 (1996).

[16] A. La Magna and R. Pucci, Phys. Rev. B **55**, 14886 (1997).

[17] C.-H. Pao and H.-B. Schttler, Phys. Rev. B **57**, 5051 (1998).

[18] L. Proville and S. Aubry, Physica D **113**, 307 (1998).

[19] K. Yonemitsu, J. Zhong, and H.-B. Schttler, Phys. Rev. B **59**, 1444 (1999).

[20] J. Bonča and S. A. Trugman, Phys. Rev. B **64**, 094507 (2001).

[21] Y. Takada and A. Chatterjee, Phys. Rev. B **67**, 081102(R) (2003).

[22] H. Fehske, G. Wellein, G. Hager, A. Weiße, and A. R. Bishop, Phys. Rev. B **69**, 165115 (2004).

[23] A. Macridin, G. A. Sawatzky, and M. Jarrell, Phys. Rev. B **69**, 245111 (2004).

[24] W. Koller, D. Meyer, A. C. Hewson, and Y. Ōno, Physica B **359**, 795 (2005).

[25] R. T. Clay and R. P. Hardikar, Phys. Rev. Lett. **95**, 096401 (2005).

[26] K.-M. Tam, S.-W. Tsai, D. K. Campbell, and A. H. Castro Neto, Phys. Rev. B **75**, 161103(R) (2007).

[27] A. F. Hebard, M. J. Rosseinsky, R. C. Haddon, D. W. Murphy, and S. H. Glarum, Nature (London) **350**, 600 (1991).

[28] K. Tanigaki, T. W. Ebbesen, S. Saito, J. Mizuki, and J. S. Tsai, Nature (London) **352**, 222 (1991).

[29] O. Gunnarsson, Rev. Mod. Phys. **69**, 575 (1997).

[30] M. Sawamura, K. Kawai, Y. Matsuo, K. Kanie, T. Kato, and E. Nakamura, Nature (London) **419**, 702 (2002).

[31] S. Okada, R. Arita, Y. Matsuo, E. Nakamura, A. Oshiyama, and H. Aoki, Chem. Phys. Lett. **399**, 157 (2004).

[32] S. R. White, Phys. Rev. Lett. **69**, 2863 (1992).

[33] S. R. White, Phys. Rev. B **48**, 10345 (1993).

[34] R. M. Noack, S. R. White, and D. J. Scalapino, Phys. Rev. Lett. **73**, 882 (1994).

[35] C. A. Hayward, D. Poilblanc, R. M. Noack, D. J. Scalapino, and W. Hanke, Phys. Rev. Lett. **75**, 926 (1995).

[36] E. Jeckelmann and S. R. White, Phys. Rev. B **57**, 6376 (1998).

[37] M. Tezuka, J. Phys. Soc. Jpn. **76**, 053001 (2007).

[38] E. Jeckelmann, C. Zhang, and S. R. White, Phys. Rev. B **60**, 7950 (1999).

[39] W. Stephan, Phys. Rev. B **54**, 8981 (1996).

[40] J. K. Freericks, M. Jarrell, and D. J. Scalapino, Phys. Rev. B **48**, 6302 (1993).

[41] M. Capone and S. Ciuchi, Phys. Rev. Lett. **91**, 186405 (2003).

[42] D. Emin and T. Holstein, Phys. Rev. Lett. **36**, 323 (1976).

[43] N. D. Mermin and H. Wagner, Phys. Rev. Lett. **17**, 1133 (1966).

[44] P. C. Hohenberg, Phys. Rev. **158**, 383 (1967).

[45] H. Shiba, Prog. Theor. Phys. **48**, 2171 (1972).

[46] Y. Nagaoka, Prog. Theor. Phys. **52**, 1716 (1974).

[47] G. Sangiovanni, M. Capone, C. Castellani, and M. Grilli, Phys. Rev. Lett. **94**, 026401 (2005).

[48] M. Capone, G. Sangiovanni, C. Castellani, and M. Grilli, Physica B **359**, 636 (2005).

[49] M. Fabrizio, Phys. Rev. B **54**, 10054 (1996).

[50] K. Kuroki, R. Arita, and H. Aoki, J. Phys. Soc. Jpn. **66**, 3371 (1997).